Available online at www.sciencedirect.com
SCIENCE DIRECT®
Talanta 64 (2004) 922–928
Talanta
www.elsevier.com/locate/talanta

Simultaneous determination of cadmium (II) and lead (II) with clay nanoparticles and anthraquinone complexly modified glassy carbon electrode

Shuai Yuan [a], Wanhua Chen [b], Shengshui Hu [a,*]

[a] *Department of Chemistry, Wuhan University, Wuhan 430072, China*
[b] *Department of Chemistry, Xianning College, Xianning 437005, China*

Received 13 January 2004; received in revised form 6 April 2004; accepted 14 April 2004
Available online 1 June 2004

Abstract

An anthraquinone (AQ) improved Na-montmorillonite nanoparticles (nano-SWy-2) chemically modified electrode (CME) has been developed for the simultaneous determination of trace levels of cadmium (II) and lead (II) by differential pulse anodic stripping voltammetry (DPASV). This method is based on a non-electrolytic preconcentration via ion exchange model, followed by an accumulation period via the complex formation in the reduction stage at −1.2 V, and then by an anodic stripping process. The mechanism of this design was proposed and the analytical performance was evaluated with several variables. Under the optimized working conditions, the detection limit was 3 and 1 nM for Cd^{2+} and Pb^{2+}, respectively. The calibration graphs were linear in the concentration ranges of 8×10^{-9} to 1×10^{-6} mol L^{-1} (Cd^{2+}) and of 2×10^{-9} to 1×10^{-6} mol L^{-1} (Pb^{2+}). Many inorganic species did not interfere with the assay significantly; the high sensitivity, selectivity, and stability of this nano-SWy-2-AQ CME were demonstrated. The applications for the detection of trace levels of Cd^{2+} and Pb^{2+} in milk powder and lake water samples indicate that it is an economical and potent method.

Keywords: Clay nanoparticles; Anthraquinone; Cadmium; Lead; Voltammetry; Chemically modified electrode

1. Introduction

Clays and their doped colloidal suspensions fabricated electrodes have been applied in electrochemical studies with abroad interest [1–4]. These electrodes are well known for their cation exchange capacity, porous surface area, high thermal and chemical stability, electrocatalytical ability, and molecular-sieving properties. Organic species and metal complexes, e.g. $M(bpy)_3^{2+}$ (bpy = 2,2′-bipyridine, M = Ru, Fe, Os), MV^{2+} (methyl viologen) are usually incorporated in the clay film and used as electrocatalysts [5–7]. However, most of the impregnated substances especially for the species located within the interlamellar region of clay are non-electroactive, since they do not contribute to the faradaic current [6,7]. It is necessary to increase the electrochemical accessibility of this region to exert fully the catalytic abilities of the clay layer [7]. Combining with an electronic conductor such as 9,10-anthraquinone (AQ) is expected to provide an "electron channel" to these inaccessible regions, as well as a metal ligand.

As the largest group of naturally occurring quinines, 9,10-anthraquinones are of fundamental importance both in industry and in medicine [8,9]. The anthraquinones have shown strong and irreversible adsorption tendency on various electrode materials [10–13]. On a preanodized GCE surface, the anthraquinones were not only simply adsorbed, but also trapped inside pores or crevices of the surface [14,15]. In recent years, some newly synthesized derivatives of 9,10-anthraquinone have been applied in the construction of chemically modified electrodes (CME) [15–17] and in the extraction membrane transport of metal ions [18,19]. As for the complex of AQ and clay colloid, however, modified glassy carbon electrode (GCE) by dropping operation has not been reported.

* Corresponding author. Tel.: +86-27-8721-8904; fax: +86-27-8764-7617.
E-mail address: sshu@whu.edu.cn (S. Hu).

0039-9140/$ – see front matter © 2004 Elsevier B.V. All rights reserved.
doi:10.1016/j.talanta.2004.04.008

Be convinced of the toxicity and hazard of cadmium and lead in the environmental and occupational fields, dose–response and legislation have been enacted to reduce human exposure to cadmium and lead [20]. The inorganic bivalent oxidation state of cadmium and lead are the most toxic in all of their related forms, and the detection of Cd^{2+} and Pb^{2+} are rigidly controlled. Anodic stripping voltammetry (ASV) is one of the most sensitive methods for the detection of trace level ions. To date, kinds of electrodes have been developed for the determination of Cd^{2+} or Pb^{2+} [21–24]. To our knowledge, detection for Cd^{2+}, Pb^{2+}, and other metal cations based on the nano-SWy-2-anthraquinone (nano-SWy-2-AQ) modified GCE or a similar system has not been reported before.

In this paper, anthraquinone solution and nano-SWy-2 colloidal suspension are cast onto the GCE surface in sequence; a complex coating is obtained via solvent evaporation. In pH 5.6 NaAc–HAc buffer solution, the differential pulse anodic stripping voltammetric (DPASV) responses of cadmium and lead increase significantly at this sandwich electrode in contrast to that at the plain GCE, or either of the single modified GCE. This assay system is satisfied with the following advantages: free mercury, low cost, excellent reproducibility, high sensitivity and selectivity.

2. Experimental

2.1. Reagents

Na-montmorillonite (SWy-2) was obtained from Source Clay Minerals Repository, University of Missouri (Columbia, MO). 9,10-Anthraquinone (Shanghai Reagent Co., China) was dissolved in acetonitrile to obtain 1×10^{-3} mol L^{-1} solution. Stock solutions of 1×10^{-2} mol L^{-1} Cd^{2+} and Pb^{2+} were prepared by dissolving $Cd(NO_3)_2$ and $Pb(NO_3)_2$ into redistilled water, and the diluted to various concentration. Other chemicals used were of analytical reagents, and used without further purification.

2.2. Apparatus

All the voltammetric measurements were carried on the CHI 830 Electrochemical analyzer (CHEN HUA Instrumental Co., Shanghai). A conventional three-electrode system comprising a saturated calomel electrode (SCE), a platinum wire auxiliary electrode, and a nano-SWy-2-AQ modified GCE (the geometric diameter of GCE is 3 mm), was employed.

Transmission electron microscopy (TEM) images were obtained using a JEM 2010 microscope (Japan). Scanning electron microscopy (SEM) was transacted with X-650 type scanning electron microscope (HITACHI, Japan). Atomic absorption spectrometry (AAS) determination was performed on 180-50 AAS (HITACHI, Japan).

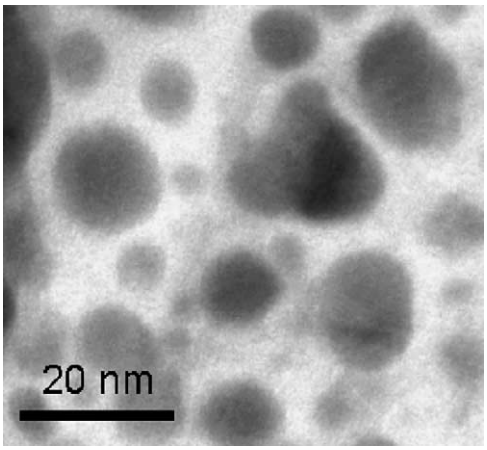

Fig. 1. TEM image of nano-SWy-2 colloidal suspension.

2.3. Preparation of the nano-SWy-2 colloid and the TEM image

The colloid of nano-SWy-2 was prepared by following steps: 30 mg SWy-2 was thoroughly dispersed in 2 mL redistilled water by continuous stirring for 12 h, and then quiescence for 5 h. After centrifugal separation at 3500 rpm for 30 min, the topper suspension was collected for experiment. The TEM image of the fresh prepared colloid is shown in Fig. 1, as can be seen that the clay particle takes on a spherical outline and the average diameter is around 10 nm.

2.4. Preparation of the modified electrode and the SEM images

The GCE was firstly polished with a 0.05 μm aluminum slurry (CHI Co.), rinsed thoroughly with redistilled water, and sonicated in water for 1 min. The GCE was preanodized by potential cyclic sweep between −0.5 and 1.5 V in 0.5 mol L^{-1} H_2SO_4 at 100 mV s^{-1} for 15 min, and rinsed with water. Then 2 μL AQ solution was cast onto the GCE surface, and dried ambiently. The prepared AQ-coating electrode was further covered with 2 μL nano-SWy-2 colloid and evaporated at room temperature in the air. The single-coating modified electrode was prepared by the alternative procedure described above. Fig. 2 depicts the distinguishable images belonging to surfaces of the single nano-SWy-2 film (a), the single AQ coating (b), and their complex film (c) covered GCE. Apparently, the formation of the complex coating was reflected on its morphology.

Considering that the newly created special groups, the adsorptive or bound anthraquinone species were remained at the preanodized GCE surface even after brief polishing with alumina on a polishing cloth, extensive polishing with sand-paper followed by prolonged soaking the GCE in NaH_2PO_4–NaOH solution (pH 10.0) is necessary in order to remove the residual anthraquinones.

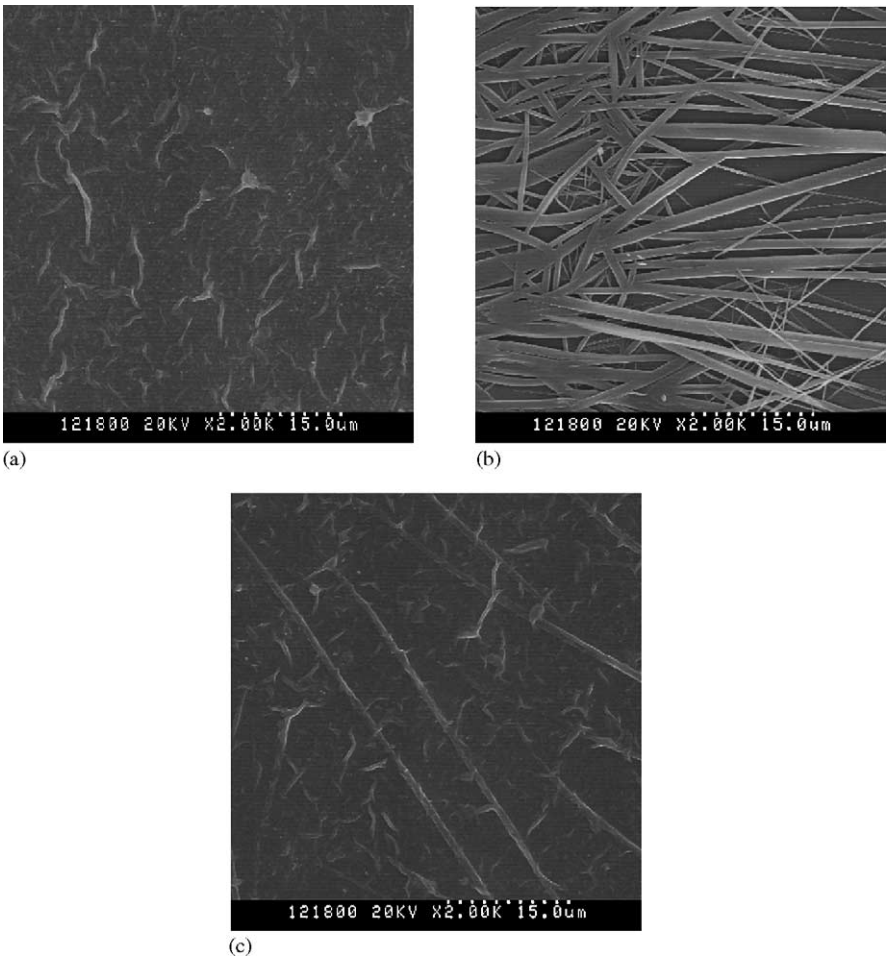

Fig. 2. SEM images of GCE surfaces modified with the nano-SWy-2 film (a), the AQ coating (b), and their complex film (c).

2.5. Analytical procedure

Unless otherwise stated, a 0.1 mol L^{-1} NaAc–HAc buffer solution was used as the supporting electrolyte for Cd^{2+} and Pb^{2+} determination. The accumulation step proceeded at −1.20 V for a selected time while the solution was stirred. The differential pulse anodic stripping voltammograms were recorded when sweep from −1.20 to −0.3 V after 15 s quiescence. The peak currents at −0.86 V for Cd^{2+} and −0.62 V for Pb^{2+} were measured. Before the repeated measurements at the same SWy-2-AQ modified GCE, the electrode was rinsed with redistilled water gently, and dried in the ambient condition.

3. Results and discussion

3.1. The reaction scheme

Clay linings, such as montmorillonite, are used as barriers to prevent subsoil and groundwater from contamination of heavy metals. The uptake of heavy metal ions by montmorillonite from solution is attributes to the ion exchange (which seems to be the main factor and dependent on the pH) and surface complexation adsorption [25]. AQ here acts as an electron-transfer accelerator besides as a metal ligand. The proposed mechanism is described as the following steps: At first, as illustrated in Fig. 3A, nano-SWy-2 film is simply a face-to-face aggregate of individual clay sheet-stacks while the AQ molecules are tiled on the GCE surface irregularly. When the modified electrode is soaking in diluted electrolyte (0.1 mol L^{-1}), the solvent uptake leads to an increase of the basal spacing and a more random orientation of the clay sheets. Under an enough negative accumulation potential (−1.20 V), AQ on the GCE surface is in the reductive form (AQH_2), and take a near-stand-up space tropism on the GCE surface with the quinohydroxyls band towards or away from the GCE surface (Fig. 3B). Such a situation is possible for the AQ molecules to intercalate into the clay inner layers by the channels between the clay particles, diffuse into the clay membrane via pinholes, or even adsorb on the clay sheets [5]. The formation of this sandwich structure obviously enlarges electron-accessible regions between the GCE surface and solution. By ion exchanging via the clay and complexing with AQH_2, Cd^{2+}, and Pb^{2+} cations in the solution are preconcentrated and reduced at the electrode

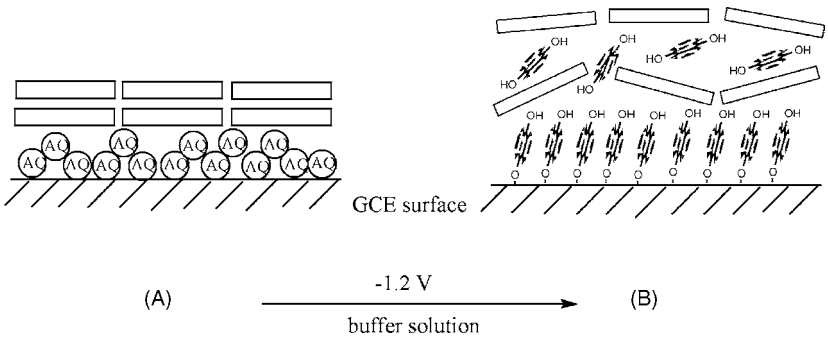

Fig. 3. Schematic of the formation of (nano-SWy-2-AQ GCE) sandwich electrode.

surface under the negative potential and the products were then oxidized in the stripping stage. The mechanism can be described as following:

$$(M^{2+})_{solution} + 2(Na^{+}X^{-})_{surface} \rightleftharpoons (M^{2+}X_2^{-})_{adsorption} + 2(Na^{+})_{solution}$$

$$(AQ)_{surface} + 2e + 2H^{+} \rightleftharpoons (AQH_2)_{surface}$$

$$(M^{2+}X_2^{-})_{adsorption} + (AQH_2)_{surface} \rightarrow (M^{2+} - AQH_2)_{adsorption} + 2(X^{-})_{surface}$$

$$(M^{2+} - AQH_2)_{adsorption} + 2e \rightarrow (M^{0} - AQH_2)_{adsorption}$$

$$(M^{0} - AQH_2)_{adsorption} \rightarrow (M^{2+})_{solution} + (AQ)_{surface} + 4e + 2H^{+}$$

where M means lead and cadmium.

3.2. Differential pulse voltammetric responses of Cd^{2+} and Pb^{2+}

Fig. 4 shows the differential pulse voltammograms of 2×10^{-7} mol L^{-1} Cd^{2+} and 1×10^{-7} mol L^{-1} Pb^{2+} at bare GCE and different modified GCEs. The response on bare GCE is poor with a small fail-shaped peak of Pb^{2+},

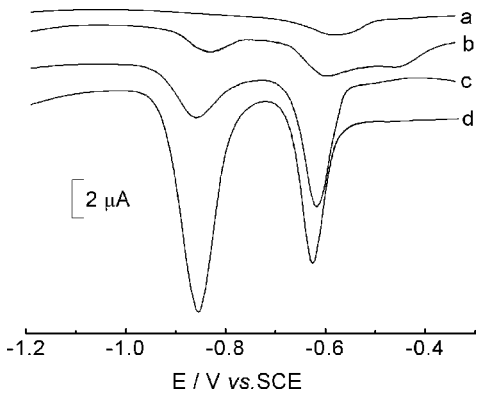

Fig. 4. Differential pulse voltammograms of 2×10^{-7} mol L^{-1} Cd^{2+} and 1×10^{-7} mol L^{-1} Pb^{2+} in pH 5.6 NaAc–HAc buffer. Accumulation potential: −1.20 V; accumulation time: 5 min; scan rate: 50 mV s^{-1}; pulse amplitude: 100 mV; pulse width: 50 ms.

even no apparent response for Cd^{2+} (a) is observed. At AQ coated GCE, two peaks at −0.86 V (Cd^{2+}) and −0.62 V (Pb^{2+}) appeared, but the stripping peak of Pb^{2+} seems to be spliced with the anodic peak of AQ group at −0.46 V (b). Under the identical conditions, the nano-SWy-2 coated GCE gives significantly increased signals at the same potentials (c), especially for Pb^{2+}. As has been illustrated previously the rate of remove lead is always higher than that of cadmium, and lead is retained more than cadmium [25]. The nano-SWy-2-AQ modified GCE inherits the enhancement at nano-SWy-2 GCE and arises a dramatic increase for Cd^{2+} (d). Besides the high sensitivity, there is almost no leaching of AQ out of the clay coating due to the low solubility of AQ in aqueous solution; the stability of this sandwich electrode is also attractive. Hence, the stripping peaks of Cd^{2+} and Pb^{2+} were investigated by differential pulse voltammetry for analytical applications.

3.3. Effect of pH

The pH variations influence the uptake mechanism, the sorption capability of Na-montmorillonite towards heavy metals, and the proton-involved reduction of AQ in aqueous solution. Adsorption of lead and cadmium by Na-montmorillonite increases with pH and reaches a plateau for the removal rates in the pH range of 3.0–6.0 [25]. Antraquinones are known to undergo a reversible two-proton and two-electron reduction in aqueous solution to give the corresponding hydroquinone derivatives. Our experiments exhibited a pH dependence of the potentials for AQ group consistent with that has been reported [15]. In the pH range investigated (pH 3.0–7.0), the redox peak potentials of AQ continuously shift toward more positive values by decreasing pH values. Compared with the stripping peaks of Cd^{2+} and Pb^{2+}, the anodic peaks of AQ always occur at more positive potentials with smaller peak currents at nano-SWy-2-AQ GCE, and do not interfere with the responses of Cd^{2+} and Pb^{2+}. However, the electrochemical responses of Cd^{2+} and Pb^{2+} vary as a function of the acidity of the electrolyte. As shown in Fig. 5, the anodic stripping voltammetric behaviors of Cd^{2+}

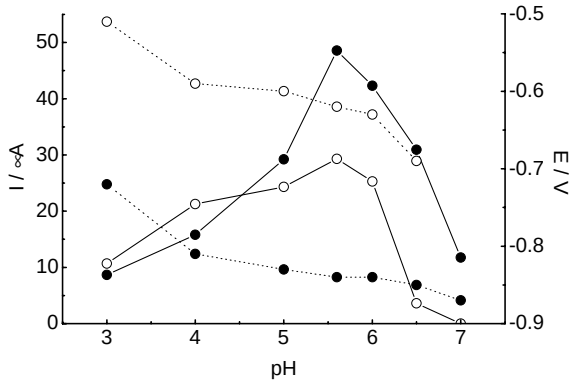

Fig. 5. Effect of pH on the stripping peak potentials (dot) and peak currents (straight) of 5×10^{-7} mol L^{-1} Pb^{2+} (hollow) and 1×10^{-6} mol L^{-1} Cd^{2+} (solid) at nano-SWy-2-AQ GCE. Others are the same as in Fig. 4.

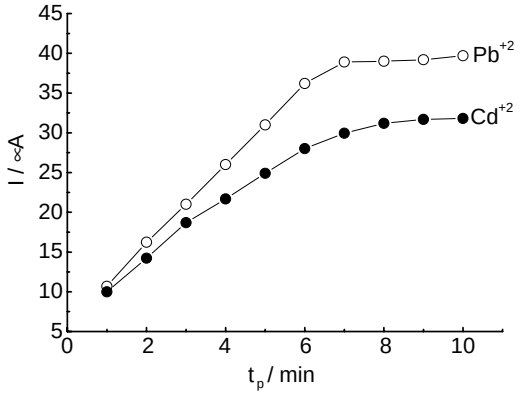

Fig. 6. Influence of accumulation time on the stripping peak currents of 5×10^{-7} mol L^{-1} Pb^{2+} (hollow) and Cd^{2+} (solid) at nano-SWy-2-AQ GCE. Others are the same as in Fig. 4.

and Pb^{2+} in 0.1 mol L^{-1} NaAc–HAc buffer solution were examined as pH changing. The fact that the stripping peak potentials of both Cd^{2+} and Pb^{2+} shift negatively with the increasing pH demonstrates the participation of proton in the electrochemical process. The stripping peak currents increased as pH up from 3.0 to 5.6, and then decreased gradually over the pH range from 5.6 to 7.0. At pH 7.0 no apparent stripping peak current of Pb^{2+} was observed attributes to the hydrolysis of Pb^{2+}. Otherwise, the stability of nano-SWy-2-AQ complex film becomes poor at pH > 7.0 or pH < 3.0. The adsorptive anthraquinone species are continuously detached from the electrode surface at high pH values, and the montmorillonite possesses a strong tendency for decreased surface area and swelling as the pH decreases.

3.4. Effect of preconcentration potential and time

The stripping peak currents increase gradually when the accumulation potential shifts from −0.90 to −1.30 V, and two well-separated stripping peaks corresponding to Cd^{2+} and Pb^{2+} were obtained with the highest peak currents as −1.30 V employed. Further negative shift of the accumulation potential led to the decreased peak currents and distorted peak shapes, which is mainly due to the co-hydrogen evolution at such negative potentials.

Under a fixed accumulation potential of −1.20 V, the stripping peak currents still improve as prolonging the preconcentration time. As shown in Fig. 6, the stripping peak currents of 5×10^{-7} mol L^{-1} Cd^{2+} and Pb^{2+} were found to increase in the first 6 min, and then level off. A further preconcentration time increase does not cause the prominent increase of the stripping peak currents. The curvature presumably suggests either a saturation loading or an equilibrium surface coverage. Therefore, the peak currents altered lightly when the accumulation time beyond 6 min. The prolongation of accumulation time is necessary for lower concentrations Cd^{2+} and Pb^{2+}.

3.5. Effect of the amounts of modifiers on the sandwich electrode

The DPASV responses of Cd^{2+} and Pb^{2+} are closely related to the thickness of the modified films on the GCE surface, which is characterized by the amounts of nano-SWy-2 and AQ. The relationship between the stripping peak currents and the volume of nano-SWy-2 colloidal suspension was investigated with 2 μL of 1×10^{-3} mol L^{-1} AQ pre-coated on GCE. The stripping peak currents of Cd^{2+} and Pb^{2+} decreased continuously when nano-SWy-2 increased from 2 to 16 μL by an interval of 2 μL. Obviously indicates that a thicker film gave a more difficult electrode response. With the volumes of nano-SWy-2 and AQ fixed as 2 μL, respectively, the concentration of AQ was optimized by varying from 5×10^{-4} to 2×10^{-3} mol L^{-1}. The plots between the Cd^{2+} and Pb^{2+} DPASV responses and AQ

Table 1
Interferences of some inorganic species on the simultaneous detection of 5×10^{-7} mol L^{-1} Cd^{2+} and Pb^{2+}

Interfering ions	Concentration (mol L^{-1})	Signal change (%)	
		Cd^{2+}	Pb^{2+}
K^+	1×10^{-3}	+0.1	+0.1
Ca^{2+}	1×10^{-3}	+0.9	+0.8
Mn^{2+}	1×10^{-3}	−1.6	−1.5
Mg^{2+}	1×10^{-3}	−1.2	−1.1
Fe^{2+}	1×10^{-4}	+2.9	+2.1
Zn^{2+}	1×10^{-4}	+2.7	+2.4
Cu^{2+}	2×10^{-5}	−3.2	−2.1
Co^{2+}	2×10^{-5}	−2.1	−3.3
Ni^{2+}	2×10^{-5}	−2.9	−2.0
Hg^{2+}	5×10^{-6}	+12.1	+9.1
SCN^-	1×10^{-3}	−1.5	−1.2
Cl^-	1×10^{-3}	−0.4	−0.6
SO_4^{2-}	1×10^{-3}	−1.2	−1.8
PO_4^{3+}	1×10^{-3}	−1.9	−2.1
NO_3^-	1×10^{-3}	+0.2	+0.3

Accumulation potential: −1.20 V; accumulation time: 5 min; scan rate: 50 mV s^{-1}; pulse amplitude: 100 mV; pulse width: 50 ms.

Table 2
Determination of Cd^{2+} and Pb^{2+} in samples ($n = 3$ for each)

Ions	Milk powder (BCR 151)		Lake water	
	Found ($\mu g\,g^{-1}$)	Certified values ($\mu g\,g^{-1}$)	This method ($mol\,L^{-1}$)	AAS ($mol\,L^{-1}$)
Cd^{2+}	$(121 \pm 14)^{a} \times 10^{-3}$	$(101 \pm 8) \times 10^{-3}$	$(6.73 \pm 0.24) \times 10^{-8}$	$(7.59 \pm 0.17) \times 10^{-8}$
Pb^{2+}	1.73 ± 0.21	2.00 ± 0.03	$(3.01 \pm 0.16) \times 10^{-8}$	$(2.85 \pm 0.23) \times 10^{-8}$

[a] Values are mean of triplicate determinations ± S.D.

concentration gave two similar parabolas. The maximum of the DPASV responses are obtained when $1 \times 10^{-3}\,mol\,L^{-1}$ AQ solution was employed.

3.6. Interferences

The possible interferences of some inorganic species are summarized in Table 1. The experimental result shows that vast of cations and anions, such as K^{+}, Ca^{2+}, Mn^{2+}, Mg^{2+} (up to $1 \times 10^{-3}\,mol\,L^{-1}$), Fe^{2+}, Zn^{2+} (each $1 \times 10^{-4}\,mol\,L^{-1}$), Cu^{2+}, Co^{2+}, Ni^{2+} (each $2 \times 10^{-5}\,mol\,L^{-1}$), SCN^{-}, Cl^{-}, $SO_4{}^{2-}$, $PO_4{}^{3+}$, $NO_3{}^{-}$ (up to $1 \times 10^{-3}\,mol\,L^{-1}$) do not arise the signals deviation of $5 \times 10^{-7}\,mol\,L^{-1}$ Cd^{2+} and Pb^{2+} larger than 4%. Only Hg^{2+} ($> 5 \times 10^{-6}\,mol\,L^{-1}$) was found to increase the determination seriously, since Hg^{2+} tends to reduce to mercury at -1.2 V and hence promote the reduction of Cd^{2+} and Pb^{2+} by the formation of amalgam. As for the reasons why the film does not suffer interference of many reducible cations, it involves several aspects. These cations can not complex with AQH_2 effectively or get deposited on the surface of the GCE because of their large overpotentials. At pH 5.6, many interfering cations hydrolyze while Cd^{2+} and Pb^{2+} do not. Moreover, nano-SWy-2 film acts as a barrier on the electrode, many anions and some cations more weakly adsorbed by the clay than Cd^{2+} and Pb^{2+}. If interfering ions of high concentration exist, CN^{-} can be added to eliminate the interferences because most potential metal ions have stronger complexing ability with CN^{-} than Pb^{2+} and Cd^{2+}.

3.7. Calibration graph and applications

Under optimum conditions, the stripping peak currents are proportional to the concentration from 8×10^{-9} to $1 \times 10^{-6}\,mol\,L^{-1}$ ($r = 0.990$) and 2×10^{-9} to $1 \times 10^{-6}\,mol\,L^{-1}$ ($r = 0.998$) for Cd^{2+} and Pb^{2+}, respectively. At 5 min preconcentration, the lowest detectable concentration of Cd^{2+} is evaluated to be 3 nM and that of Pb^{2+} is to be 1 nM.

The precision of this determination system was demonstrated by repeated analysis of a standard Cd^{2+} and Pb^{2+} solution of $5 \times 10^{-7}\,mol\,L^{-1}$. For detections performed at the same nano-SWy-2-AQ modified GCE, the relative standard deviations (R.S.D.) are 3.2 and 2.1% ($n = 5$). In the case that the modified electrode was remade every time, the R.S.D are 3.4 and 2.9% ($n = 5$), respectively. The long-term stability was estimated by recording stripping voltammograms of Cd^{2+} and Pb^{2+} at the same modified electrode every other day over half a month, the maximum deviation obtained are 5.0% for Cd^{2+} and 4.6% for Pb^{2+}. These results suggest the excellent reproducibility of this sandwich electrode.

To evaluate its accuracy in the practical applications, the nano-SWy-2-AQ modified GCE was employed to determinate Cd^{2+} and Pb^{2+} in milk powder (BCR 151) and lake water samples. For the analysis of milk powder, 500 mg solid sample was digested with HNO_3–$HClO_4$ (6 + 1, v/v) to near-dryness, 20 mL redistilled water was added in the residue and evaporated to dry again for removing the residual acids. The residue was dissolved with pH 5.6 NaAc–HAc buffer for measurement directly. The water samples were from a lake near a residential area, and analyzed without pretreatment. The electrochemical experimental results correlated well with the certified values or with those obtained by the atomic absorption spectrometry. The comparison is listed in Table 2 and indicates that the nano-SWy-2-AQ modified GCE is potent for the practical sample analysis.

4. Conclusion

Na-montmorillonite was dispersed with water to obtain the nanoparticles. The conventional clay colloidal suspension was tentatively combined with functional organic species 9,10-anthraquinone. Based on this, a novel and effective electrode system was developed. Measurements of Cd^{2+} and Pb^{2+} in aqueous solution were carried out with this chemically modified GCE by using DPASV. The optimized working conditions were described. Combining the ion exchange capability of clay with the electronic conductor function of AQ, a sensitive electrochemical technique for the simultaneous determination of Cd^{2+} and Pb^{2+} has been developed.

Acknowledgements

The authors appreciate the support from the National Science Foundation of China (Nos. 60171023 and 30370397).

References

[1] P.K. Ghosh, A.J. Bard, J. Am. Chem. Soc. 105 (1983) 5691.
[2] N. Oyama, F.C. Anson, J. Electroanal. Chem. 199 (1986) 467.

[3] C.V. Kumar, G.L. McLendon, Chem. Mater. 9 (1997) 863.
[4] X. Chen, N. Hu, Y. Zeng, J.F. Rusling, J. Yang, Langmuir 15 (1999) 7022.
[5] D. Ege, P.K. Ghosh, J.R. White, J.F. Equey, A.J. Bard, J. Am. Chem. Soc. 107 (1985) 5644.
[6] W.E. Rudzinski, A.J. Bard, J. Electroanal. Chem. 199 (1986) 323.
[7] W.E. Rudzinski, C. Figueroa, C. Hoppe, T.Y. Kuromoto, D. Root, J. Electroanal. Chem. 243 (1988) 367.
[8] R.H. Thomson, Naturally Occurring Quinones, Academic Press, New York, 1971.
[9] N.J. Lowe, R.E. Ashton, H. Koudsi, M. Verschoore, H. Schaefer, J. Am. Acad. Dermatol. 10 (1984) 69.
[10] P. He, R.M. Crooks, L.R. Faulkner, J. Phys. Chem. 94 (1990) 1135.
[11] M.P. Soriaga, A.T. Hubbard, J. Am. Chem. Soc. 104 (1982) 2735.
[12] J. Zhang, F.C. Anson, J. Electroanal. Chem. 331 (1992) 945.
[13] T.M. Mohan, H. Gomathi, G.P. Rao, Bull. Electrochem. 6 (1990) 630.
[14] H. Gomathi, G.P. Rao, J. Electroanal. Chem. 85 (1985) 190.
[15] A. Salimi, H. Eshghi, H. Sharghi, S.M. Golabi, M. Shamsipur, Electroanalysis 11 (1999) 114.
[16] S. Hu, C. Xu, G. Wang, D. Cui, Talanta 54 (2001) 115.
[17] M.F. Mousavi, A. Rahmani, S.M. Golabi, M. Sharmsipur, H. Sharghi, Talanta 55 (2001) 305.
[18] S. Dadfarnia, M. Shamsipur, F. Tamaddon, H. Sharghi, J. Membr. Sci. 78 (1993) 115.
[19] M.F. Mousavi, S. Sahari, N. Alizadeh, M. Sharmsipur, Anal. Chim. Acta 414 (2000) 189.
[20] A.D. Ibrahim, A.B. Diane, Anal. Chem. 74 (2002) 52.
[21] O. Acar, Talanta 55 (2001) 613.
[22] C. Hu, K. Wu, X. Dai, S. Hu, Talanta 60 (2003) 17.
[23] J. Wang, J. Lu, S.B. Hocevar, P.A.M. Farias, Anal. Chem. 72 (2000) 3218.
[24] Y. Bonfil, M. Brand, E. Kirowa-Eisner, Anal. Chim. Acta 464 (2002) 99.
[25] F. Barbier, G. Duc, M. Petit-Ramel, Colloids Surf. A 166 (2000) 153.